ELSEVIER

European Journal of Pharmacology 393 (2000) 197–204

ejp

www.elsevier.nl/locate/ejphar

Molecular characterization of the specificity of interactions of various neurotoxins on two distinct nicotinic acetylcholine receptors

Denis Servent [a,*], Stéphanie Antil-Delbeke [a], Carole Gaillard [a], Pierre-Jean Corringer [b], Jean Pierre Changeux [b], André Ménez [a]

[a] *CEA / Saclay, Département d'Ingénierie et d'Etudes des Protéines, 91191 Gif-sur-Yvette, France*
[b] *Laboratoire de Neurobiologie Moléculaire, Institut Pasteur, 75724 Paris Cedex 15, France*

Accepted 21 January 2000

Abstract

Snake curaremimetic toxins are currently classified as short-chain and long-chain toxins according to their size and their number of disulfide bonds. All these toxins bind with high affinity to muscular-type nicotinic acetylcholine receptor, whereas only long toxins recognize the α7 receptor with high affinity. On the basis of binding experiments with *Torpedo* or neuronal α7 receptors using wild-type and mutated neurotoxins, we characterized the molecular determinants involved in these different recognition processes. The functional sites by which long and short toxins interact with the muscular-type receptor include a common core of highly conserved residues and residues that are specific to each of toxin families. Furthermore, the functional sites through which α-cobratoxin, a long-chain toxin, interacts with muscular and α7 receptors share similarities but also marked differences. Our results reveal that the three-finger fold toxins have evolved toward various specificities by displaying distinct functional sites.

Keywords: Nicotinic acetylcholine receptor; Neurotoxin; α-Cobratoxin

1. Introduction

Curaremimetic toxins isolated from snake venoms can be divided into two major subfamilies on the basis of both amino acid sequences (Endo and Tamiya, 1991) and functional properties (Servent et al., 1997). One subfamily involves the long-chain toxins with 66–74 residues and five disulfide bonds, which bind with high affinities to both muscular-type and neuronal α7 nicotinic receptors (Endo and Tamiya, 1991; Servent et al., 1997). The other subfamily involves short-chain toxins with 60–62 residues and four disulfide bonds, which bind with high affinity on muscular-type nicotinic acetylcholine receptors only. Preliminary data indicated that the specificity of the long-chain toxins for the α7 receptor may be associated with the presence of a fifth disulfide bond at the tip of their central loop (Servent et al., 1997). Therefore, curaremimetic toxins do not form a family of functionally homogeneous proteins. To understand the molecular mechanisms involved in their differential interaction capacities, we have elucidated on one hand the sites by which short-chain and long-chain toxins bind to muscular-type receptor and on the other hand the binding site of the long-chain α-cobratoxin for muscular and α7 receptors. To approach this question, we expressed this toxin in *E. coli*, submitted it to extensive mutational analysis, and observed the effect of these mutations on both receptor subtypes.

The data obtained indicate that long-chain and short-chain toxins recognize muscular-type receptor by using first a common binding core consisting mainly of positively charged and aromatic residues, but also specific residues that may provide each toxin with a unique binding profile. Furthermore, our results demonstrate that α-cobratoxin recognizes the two receptor subtypes with six

* Corresponding author. Tel.: +33-1-690-85202; fax: +33-1-690-89137.
E-mail address: denis.servent@cea.fr (D. Servent).

0014-2999/00/$ - see front matter
PII: S0014-2999(00)00095-9

identical residues (Trp[25], Asp[27], Phe[29], Arg[33], Arg[36], and Phe[65]) assisted by additional residues which bind selectively to muscular (Lys[23] and Lys[49]) or α7 (Ala[28], Cys[26]–Cys[30], and Lys[35]) receptors.

2. Materials and methods

2.1. Expression, purification, and characterization of recombinant α-cobratoxin

Recombinant wild-type and mutant α-cobratoxin were obtained as previously described (Antil et al., 1999). Briefly, cDNA encoding cobratoxin was cloned into the pCP vector (Drevet et al., 1997) and expressed as a fusion protein in the BL21(DE3) *E. coli* strain. The fused toxin was purified on an Immunoglogulin G-Sepharose column, cleaved by CNBr, refolded with GSH/GSSG (4/2 mM) and purified on a reverse phase (C4) column. The α-cobratoxin mutants described here were prepared using the Stratagene kit (Quick Change) and the sequence of the entire gene was checked by automatic sequencing (ABI PRISM™ 310 Genetic Analyses, Applied Biosystem Perkin Elmer). Biochemical and biophysical characterization of each mutant was done by (i) sodium dodecyl sulfate polyacrylamide gel electrophoresis (SDS-PAGE) with silver staining, (ii) analytical reverse phase chromatography (HPLC), (iii) electrospray mass spectroscopy and circular dichroic analysis, as previously described (Antil et al., 1999). The concentration of purified cobratoxin was determined by measuring the absorbance at 278 nm of a given solution of toxin and amino acid analysis.

2.2. Expression of α7 receptor in human embryonal kidney (HEK) cells

A chimeric cDNA of a neuronal type nicotinic receptor (α7-5-HT_3) was transfected into HEK 293 cells by calcium precipitation as described previously (Eiselé et al., 1993; Corringer et al., 1995; Servent et al., 1997). Two days after the transfection, the cells were harvested in a phosphate-buffered saline (PBS) with 5 mM EDTA, washed twice with PBS, and finally resuspended in 3 ml/plate of this buffer for the binding experiments.

2.3. Binding assays

Competition experiments with nicotinic acetylcholine receptor from *T. marmorata* were performed at equilibrium, using [^{3}H]toxin α as a radioactive tracer, as previously described (Antil et al., 1999). Different concentrations of α-cobratoxin were incubated with 1 pmol of toxin binding sites and 6.4 nM [^{3}H]toxin α for at least 4 h at 20°C, and the mixture was filtered through Millipore filters (HAWP) which had been soaked in Ringer buffer. The filters were washed with 6 ml of Ringer buffer, dried, and after the addition of 10 ml of scintillation solution (Lipoluma), were counted on a Rackbeta counter (Amersham Pharmacia Biotech). Binding measurements were analysed first by the empirical Hill equation in order to define the Hill coefficient which could be correlated to the presence of one ($n_H = 1$) or two binding sites (n_H less than unity). Afterward, the functions describing competitive binding of α-cobratoxin mutants to either a single site or two independent sites were fitted by non-linear regression. Statistical improvement in the computer fit for a two-site model versus a one-site model was determined by the extra sum of squares principle, utilizing the *F*-test. The two-site model was accepted when the statistical comparison between the two models gave a value of $P < 0.05$. The IC_{50} values determined by non-linear regression analysis were converted to apparent dissociation constant values (K_d) as described by Cheng and Prusoff (1973). All these fits and statistical analyses were performed using Prism software (GraphPad).

The affinities of the toxins for the α7-5-HT_3 receptor were determined as previously described (Servent et al., 1997, 1998). Competition experiments showed the effect of wild-type and mutated recombinant α-cobratoxin on the initial rate of ^{125}I-Bgtx binding. Different concentrations of α-cobratoxin were preincubated with cell suspension under equilibrium, and filtered 6 min after the addition of 5 nM ^{125}I-Bgtx. The protection constant (K_p) calculated by fitting the competition data to the empirical Hill equation was shown to correspond to the dissociation constants (Weber and Changeux, 1974; Corringer et al., 1995).

3. Results

3.1. Selection of α-cobratoxin mutants

The recombinant toxins, wild-type or mutated, were characterized by their physico-chemical properties (sequence analyses, CD spectra, electrospray mass analyses) and the final yield of their production varied from 0.5 to 1.2 mg/l of culture.

Based on both the three-dimensional structure homology between long-chain and short-chain toxins, especially at their second and third loops (Tsernoglou and Petsko, 1977; Walkinshaw et al., 1980; Low and Corfield, 1986; Zinn Justin et al., 1992) and on the previous characterization of the site through which short-chain toxins interact on the *Torpedo* receptor (Pillet et al., 1993; Trémeau et al., 1995; Ackermann and Taylor, 1997), we first probed the role of structurally homologous residues in α-cobratoxin. Then, we proceeded to the mutations K23E, W25H, W25F, W25A, D27N, D27R, R33E, D38L, and K49E. In addition, we explored the possible involvement of the structural differences between short and long toxins in their interaction on the *Torpedo* receptor by mutating extensively the first loop, the tip of loop II, and the C-terminal tail of α-cobratoxin.

3.2. Effect of the mutations of α-cobratoxin on its interaction on the Torpedo receptor

Binding affinities of native and wild-type or mutated recombinant α-cobratoxin for *Torpedo* receptor were determined on the basis of competition experiments, using [^{3}H]toxin α as a radioactive tracer. Typical competition binding curves are shown in Fig. 1A and dissociation constants deduced from these curves are equal to 39 and 58 pM for native and recombinant α-cobratoxine, respectively. With two exceptions, all the binding curves obtained with the wild-type or mutated toxins were characterised by Hill coefficients equal to 1.1 ± 0.2, indicating similar affinities for the two receptor binding sites. In contrast, the Hill coefficients calculated with the mutants, K23E and K49E, were equal to 0.6 ± 0.1, suggesting that

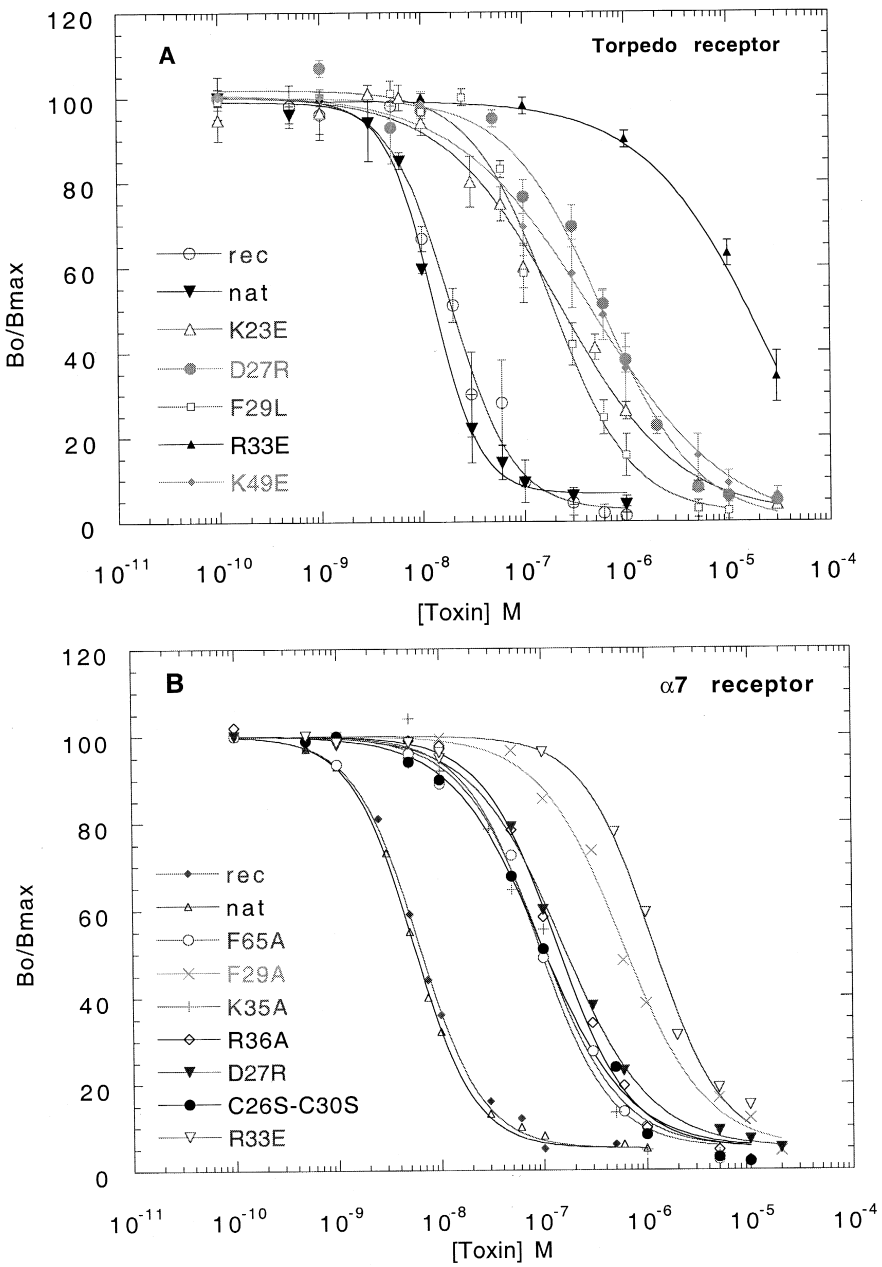

Fig. 1. Equilibrium binding of wild-type and α-cobratoxin mutants to the *Torpedo* (A) or α7-5-HT$_3$ (B) receptors. (A) Competition experiments with nicotinic acetylcholine receptor from *T. marmorata* were performed at equilibrium, using [^{3}H]toxin α as a radioactive tracer, as described in Section 2. Binding measurements were analysed by the empirical Hill equation in order to define the Hill coefficient. Then, the functions describing competitive binding of α-cobratoxin mutants to either a single site or two independent sites were fitted by non-linear regression. Statistical improvement in the computer fit for a two-site model versus a one-site model was determined by the *F*-test. The two-site model was accepted when the statistical comparison between the two models gave a value of $P < 0.05$. (B) Competition experiments showed the effect of wild-type and mutated recombinant α-cobratoxin on the initial rate of ^{125}I-bungarotoxin binding as described in Section 2. The continuous lines correspond to theoretical concentration responses fitted through the data points using the non-linear Hill equation.

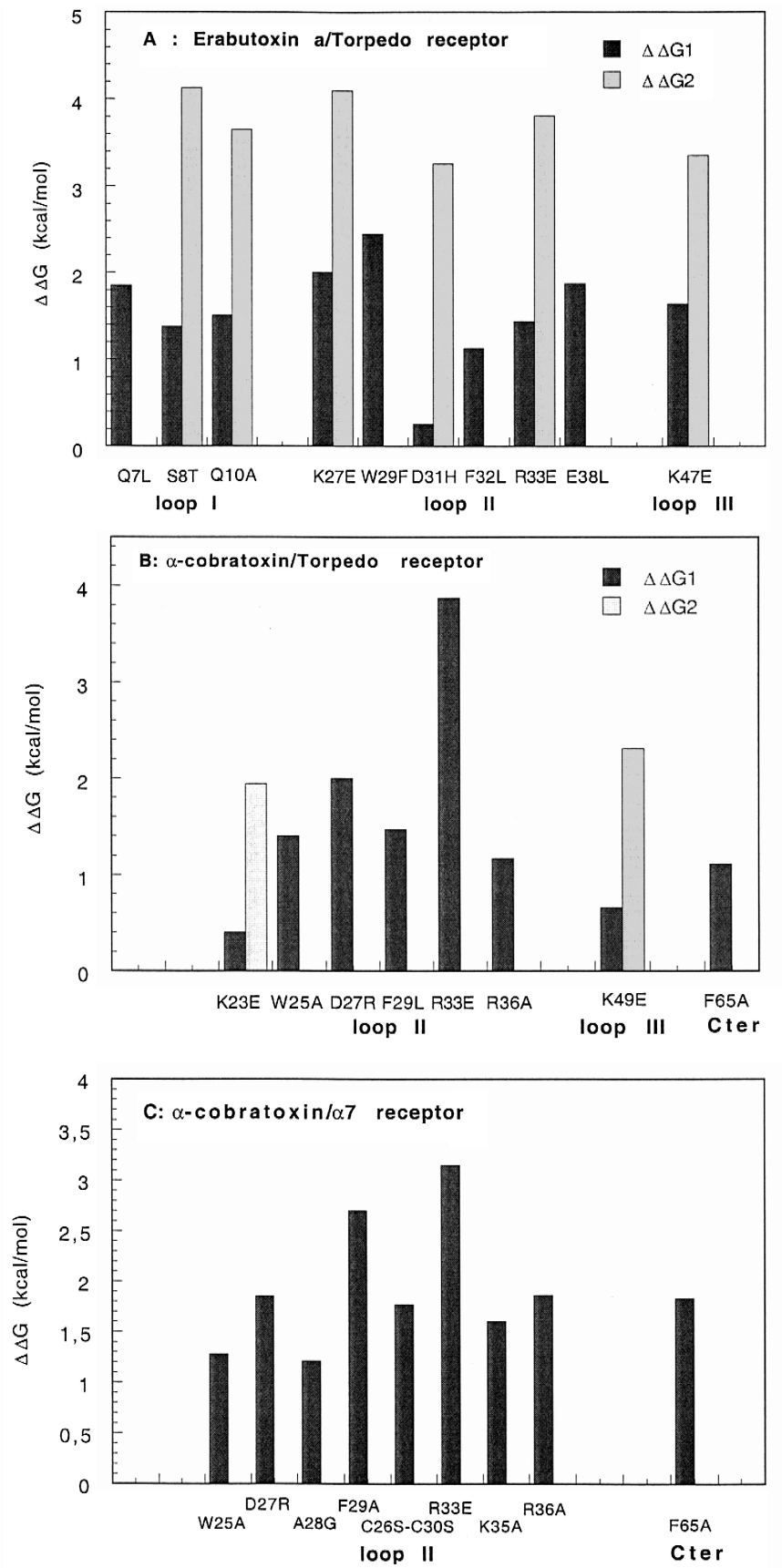
A : Erabutoxin a/Torpedo receptor
ΔΔG1
ΔΔG2
ΔΔG (kcal/mol)
0
1
2
3
4
5
Q7L S8T Q10A K27E W29F D31H F32L R33E E38L K47E
loop I
loop II
loop III
B: α-cobratoxin/Torpedo receptor
ΔΔG1
ΔΔG2
ΔΔG (kcal/mol)
0
1
2
3
4
K23E W25A D27R F29L R33E R36A K49E F65A
loop II
loop III
Cter
C: α-cobratoxin/α7 receptor
ΔΔG (kcal/mol)
0
0,5
1
1,5
2
2,5
3
3,5
4
W25A D27R A28G F29A C26S-C30S R33E K35A R36A F65A
loop II
Cter

they interact differentially with the two receptor binding sites. Statistical comparison of the fit obtained assuming an interaction on one or two binding sites indicated that the binding of K23E and K49E fits with the presence of two distinct classes of sites ($P < 0.01$). Similar differential binding may also take place for the mutant R33E, however the incomplete binding curve did not allow us to reach a convincing conclusion.

The Fig. 2B shows the difference in energy of binding at the two toxin binding sites ($\Delta\Delta G_1$, $\Delta\Delta G_2$) deduced from competition curves for all the functional residues. The mutations W25A, D27R, F29L, and R33E are characterized, respectively, by $\Delta\Delta G$ values of approximately 1.4, 2, 1.5, and 3.9 kcal/mol, suggesting the major role of Arg33 in the toxin–receptor interaction. K23E and K49E induced a significant affinity decrease at only one site with $\Delta\Delta G$ equal to 1.9 and 2.3 kcal/mol, respectively. Neither of the mutations made in the loop II on residues Tyr^{21}, Ala^{28}, Cys^{26}–Cys^{30}, Ser^{31}, Lys^{35}, and Asp^{38} caused a significant affinity decrease on the *Torpedo* receptor, suggesting that these highly conserved residues in the long-chain toxin sequences contribute little if anything to the interaction of α-cobratoxin with *Torpedo* receptor. The R36A mutation caused a small affinity decrease, which could reflect a complementary function of this residue. None of all the mutations that were introduced in the first loop, from Phe^4 to Asp^{13}, caused any effect on the toxin affinity for the *Torpedo* receptor, suggesting that this loop is not implicated in the functional site of α-cobratoxin. Finally, neither the P66A mutation nor the deletion of the five terminal residues (Δ66 mutant) caused a substantial effect on receptor recognition whereas the F65A mutation induced a weak affinity decrease with a difference in free energy of binding equal to 1.1 kcal/mol (Fig. 2B).

3.3. Effect of the mutations of α-cobratoxin on its interaction on the neuronal α7 receptor

We investigated the capacity of wild-type and mutant toxins to inhibit the binding of [^{125}I]-Bgtx to a chimeric version of the α7 chicken receptor as previously described (Servent et al., 1997). Inhibition binding curves are shown in Fig. 1B for both the wild-type and some mutated toxins which produce a significant affinity decrease. Binding affinities of α-cobratoxin for neuronal α7 receptors were deduced from the inhibition binding curves and were fitted with the Hill equation. Therefore, the wild-type recombinant α-cobratoxin and the venom toxin seem to be characterized by similar K_d values, around 6 nM, confirming the identity of the recombinant and venom toxins.

We explored the effects of mutations on various residues located on the toxin loops I, II, and III, as well as on its C-terminal tail. None of the mutations introduced in the first loop caused a significant affinity decrease, indicating that none of the residues of the first loop plays a major binding role with the neuronal α7 receptor. In contrast, nine residues of loop II, Trp^{25}, Asp^{27}, Ala^{28}, Phe^{29}, Cys^{26}–Cys^{30}, Arg^{33}, Lys^{35}, and Arg^{36}, were highly sensitive to mutations, with affinity decreases ranging from 6- to 250-fold (Fig. 1B and Fig. 2C). Six of these residues, Trp^{25}, Asp^{27}, Ala^{28}, Phe^{29}, Arg^{33}, and Arg^{36}, have their side chain essentially accessible from the concave face. The side chain of the other mutation-sensitive residues in loop II, Cys^{26}–Cys^{30}, and Lys^{35} point toward the convex face of the ß-sheet. This result indicates that both faces of the sheet of loop II are involved in the binding of α-cobratoxin to the α7 receptor in contrast to what was observed for its interaction with the *Torpedo* receptor.

Tyr^{21} and Lys^{23} of loop II and Lys^{49}, Thr^{47}, and Asp^{53} of loop III do not seem to be involved in the recognition of the α7 receptor since their mutation caused no effect on toxin affinity. Similarly, the P66A mutation or the deletion of the whole 67–71 stretch (mutant Δ66) caused no substantial effect on toxin binding affinity, in contrast, the F65A mutation caused a significant affinity decrease characterized by a $\Delta\Delta G$ equal to 1.8 kcal/mol (Fig. 2C).

In conclusion, 10 residues, Trp^{25}, Asp^{27}, Ala^{28}, Phe^{29}, Cys^{26}–Cys^{30}, Arg^{33}, Lys^{35}, Arg^{36}, and Phe^{65}, are mutation-sensitive and are likely to be involved in the interaction of α-cobratoxin on the neuronal α7 receptor, whereas a large number of surrounding residues are mutation-insensitive and hence probably excluded from the binding surface.

4. Discussion

Examination of the residues that are functionally important in the binding with the *Torpedo* receptor (Fig. 1A and Fig. 2B) allowed us to delineate an interacting surface of approximately 880 Å which crosses essentially the second and third loops (Fig. 3). The functional residues are mainly positively charged with Lys^{23}, Arg^{33}, Arg^{36}, and Lys^{49} or aromatic as Trp^{25}, Phe^{29}, and Phe^{65}. The differential effect of the K23E and K49E mutations on the toxin affinity toward the *Torpedo* receptor indicates that these two lysines do not interact similarly on the two-receptor binding sites. The incomplete binding curve obtained with the R33E mutant did not allow us to conclude definitively about the discriminative interaction of this residue. Several regions

Fig. 2. Difference in free energy of binding to the *Torpedo* receptor after mutations of functional residues on erabutoxin a (A) and α-cobratoxin (B). The results on erabutoxin a are from previous experiments (Pillet et al., 1993; Trémeau et al., 1995). $\Delta\Delta G_1$ and $\Delta\Delta G_2$ represent the difference in free energy obtained for some mutants at the two toxin binding sites. (C) Difference in free energy of binding to the neuronal α7-5-HT3 receptor for some α-cobratoxin mutants.

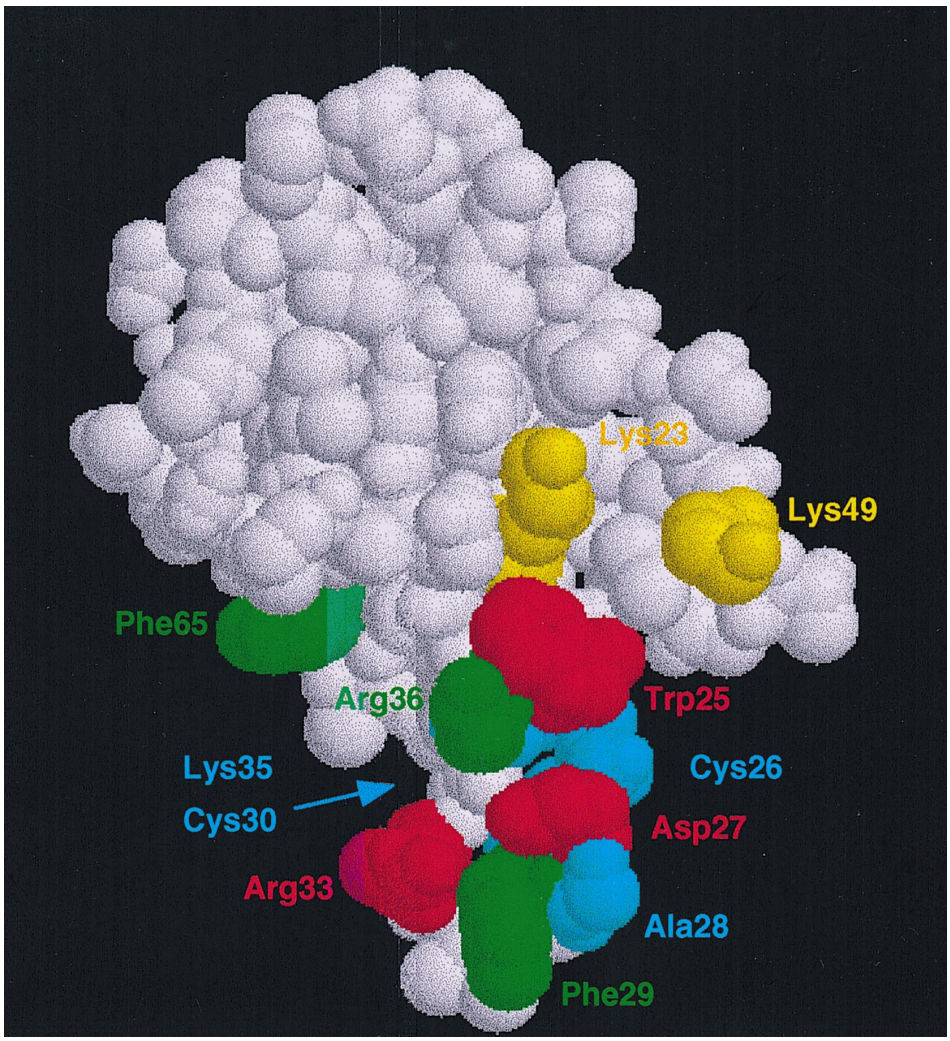

Fig. 3. Functional sites by which α-cobratoxin interacts with the *Torpedo* or α7 receptor subtypes. Residues whose mutations caused a significant and similar affinity decrease for both receptor subtypes are colored in red and those for which the mutation provoke an affinity decrease higher for α7 than for the *Torpedo* receptors are in green. Residues specifically involved in the binding to the muscular-type receptor are colored yellow, whereas, those specific in the α7 interaction are in blue.

of the toxin are excluded from the interactive surface, such as loop I which is completely insensitive to mutations, the upper part of the central loop and the end of the C-terminal tail (Fig. 3). The lack of functionality of the first loop was surprising in view of the presence of some residues highly conserved in the long-chain toxin sequences and the functional role of residues of the α-bungarotoxin loop I in its interaction with a receptor fragment (Tα185-196) as visualized by nuclear magnetic resonance (NMR) (Basus et al., 1993). However, α-bungarotoxin is an atypical long-chain toxin, especially concerning the sequence of its first loop and it is not certain that the result obtained with a receptor fragment can be extrapolated to the whole receptor.

Our results allowed us to examine how a long-chain toxin and a short-chain toxin interact with high affinity on the same target, i.e. the *Torpedo* receptor. The effects of the same mutation on identical or similar residues of erabutoxin a and α-cobratoxin are compared in Fig. 2A and B, respectively. A number of these functionally important residues are identical in nature and located at homologous positions in the two toxins. These are in erabutoxin a and α-cobratoxin, respectively, Lys^{27}/Lys^{23}, Trp^{29}/Trp^{25}, Asp^{31}/Asp^{27}, Phe^{32}/Phe^{29}, Arg^{33}/Arg^{33}, and Lys^{47}/Lys^{49}. These residues are also conserved in most other short-chain and long-chain toxins, and hence may constitute a common functional core for most curaremimetic toxins.

In addition to their remarkable functional similarities, the two toxins display a number of differences that can be appreciated at different levels. Thus, mutations at homologous residues of the functional core may not have fully identical functional consequences. This is the case for the positively charged residues. Recent analysis performed with recombinant mouse muscle receptor subunits expressed in HEK cells indicated that the two sites can be differentiated by mutations at some of these residues

(Ackermann and Taylor, 1997). In our case, some site-selectivity was identified from binding competition curves for mutants K23E and K49E of α-cobratoxin (Fig. 1A) and probably with the R33E mutant. When reviewing our previous competition data obtained with erabutoxin a mutants (Pillet et al., 1993; Trémeau et al., 1995), we noted that the two binding sites could also be discriminated with the Ea mutants S8T, Q10A, K27E, D31H, R33E, and K47 (Fig. 2A). Thus, although the discriminating factors, calculated with the mutation introduced at position Lys^{27}/Lys^{23} or Lys^{47}/Lys^{49} in erabutoxin a or cobratoxin, are highly similar, the binding energy differences associated with mutations K27E and K47E in the short-chain toxin are substantially greater than those of K23E and K49E introduced in the long-chain one (Fig. 2A and B). These observations suggest that the two critical lysines of the two toxins do not have strictly identical interactions with the two binding sites on the *Torpedo* receptor. Therefore, although the two toxins rely on a core of identical homologous residues for binding to the same target, these residues may perceive differential local environments and hence might not play strictly identical binding functions.

A number of other residues was clearly sensitive to mutations in one toxin only. This is the case for Glu^{38} which is functional in erabutoxin a only, and for Phe^{65} in the C-terminal tail which plays a complementary role in the binding of α-cobratoxin (Fig. 2A and B).

The most striking difference observed between the two toxins concerned their first loop. Three residues at the tip of this loop are crucial for the interaction of erabutoxin a on the receptor (Pillet et al., 1993; Trémeau et al., 1995) whereas all residues in the corresponding loop in α-cobratoxin are insensitive to mutations (Fig 2B). The first loop is substantially longer in the short toxin, precluding superimposition with that of the long toxin, and we suggest that the shortness of the first loop in α-cobratoxin makes its residues inaccessible to the interactive receptor surface.

To summarize, long and short curaremimetic toxins exploit, a common core composed mainly of positively charged and aromatic residues which interact with one or both toxin binding sites of the *Torpedo* receptor. However, these toxins also display marked functional differences that can be perceived at two levels. First, the binding energy contribution of some residues of the common core may be different in the two toxin families. Second, additional residues may be functionally important in one toxin only. Therefore, two curaremimetic toxins recognize the same receptor with comparably high affinities through variations around a common binding core.

Using the toxin mutants previously described, we also identified the residues by which α-cobratoxin interacts on the neuronal α7 receptor. The mutations of 10 residues of α-cobratoxin, Trp^{25}, Cys^{26}–Cys^{30}, Asp^{27}, Ala^{28}, Phe^{29}, Arg^{33}, Lys^{35}, Arg^{36}, and Phe^{65}, caused a significant affinity decrease on the neuronal α7 receptor (Fig. 1B). Numerous surrounding residues in loop I (from Phe^{4} to Asp^{13}), at the base of loop II (Tyr^{21}, Lys^{23}, and Asp^{38}), and in loop III (Thr^{47}, Lys^{49}, and Asp^{53}) are mutation-insensitive, and therefore, are probably excluded from the binding surface. With the exception of Phe^{65} in the C-terminal tail, all the functionally important residues belong to the toxin loop II, with Trp^{25}, Asp^{27}, Ala^{28}, Phe^{29}, Arg^{33}, and Arg^{36} having their side chain oriented toward the concave face, whereas those of Lys^{35} and Cys^{26}–Cys^{30} are accessible from the other face. Thus, the toxin seems to utilize its two faces to interact with the neuronal receptor. It is interesting to note the presence of three positively charged residues, Arg^{33}, Lys^{35}, and Arg^{36}, in the functional toxic site with Arg^{33} playing the most critical binding role. This positively charged cluster is surrounded by numerous hydrophobic side chains, including three aromatic residues Trp^{25}, Phe^{29}, and Phe^{65}, and one aliphatic residue Ala^{28}. Therefore, the determinant that ensures the interaction of α-cobratoxin with the α7 receptor is compactly located on the toxin central loop, with three positive charges surrounded by a hydrophobic ring.

A major goal of this study was to understand how α-cobratoxin can recognize two subsets of nicotinic acetylcholine receptors. We can now compare the functional sites through which this toxin interacts on both neuronal and *Torpedo* receptors. These results are summarized in Fig. 3 where two families of residues appeared, those for which mutation affects toxin binding affinity for both types of receptors (in red and green), and those for which mutation affects binding affinity for only one type of receptor (in yellow and blue). In this comparison, we have considered the mutational effects on one or both of the two toxin binding sites that are present in the *Torpedo* receptor. Six toxin residues were mutation-sensitive toward both receptors. These are Trp^{25}, Asp^{27}, and Arg^{33} which affect comparably the binding to both receptors (residues in red in Fig. 3) and Phe^{29}, Arg^{36}, and Phe^{65} which caused higher affinity decreases toward the α7 receptor (residues in green in Fig. 3). Therefore, the mutation data suggest that Arg^{33}, Asp^{27}, and Trp^{25} may play similar binding functions toward the *Torpedo* and neuronal receptors, and hence, might recognize similar receptor determinants. Arg^{36}, Phe^{29}, and Phe^{65} seem to contribute differently in terms of binding energy toward each receptor, suggesting that they may not have strictly identical receptor determinants.

As further indication that the toxin binding sites in the two receptors are not identical, we found a number of residues whose mutations affected only one of the two receptors. The K23E and K49E mutations affected only the binding to one site of the *Torpedo* receptor (residues in yellow in Fig. 3), indicating that the two highly conserved residues Lys^{23} and Lys^{49} are uniquely important for the curaremimetic toxins to recognize the low-affinity binding site of the muscular receptor, perhaps at the interface of the αγ subunits as previously suggested (Ackermann and Taylor, 1997; Ackermann et al., 1998). In contrast, Ala^{28},

Cys^{26}–Cys^{30}, and Lys^{35} are involved in the selective binding to the α7 receptor. We may note that Lys^{35} and the disulfide bond Cys^{26}–Cys^{30} have their side chains pointing toward the convex face of the toxin which is not considered to be functionally important in the interaction with the muscular receptor (Pillet et al., 1993; Trémeau et al., 1995; Ackermann and Taylor, 1997; Antil et al., 1999). These data may explain the origin of this differential behavior between short and long toxins on the α7 receptor. Thus, α-cobratoxin possesses a number of α7-specific residues, Ala^{28}, the disulfide bond 26–30, Lys^{35} and Phe^{65}, which tend to be highly conserved in long toxins and are lacking in short toxins (Endo and Tamiya, 1991). Some of these neuronal-specific determinants correspond to major structural deviations of long toxins, i.e. a small additional loop in the central loop and a longer C-terminal tail, and we wish to suggest that the difference in biological behavior between short and long toxins may be predominantly linked to the structural deviations between the two toxin families.

In summary, this work reveals that a toxin can recognize two different subsets of nicotinic acetylcholine receptors with a common binding core assisted by additional residues that are specific for each receptor subtype. This finding may be useful in the design of new toxins with predetermined specificity.

References

Ackermann, E.J., Ang, E.T.H., Kanter, J.R., Tsigelny, I., Taylor, P., 1998. Identification of pairwise interactions in the α-neurotoxin–nicotinic acetylcholine receptor complex through double mutant cycles. J. Biol. Chem. 273, 10958–10964.

Ackermann, E.J., Taylor, P., 1997. Nonidentity of the α-neurotoxin binding sites on the nicotinic acetylcholine receptor revealed by modification in α-neurotoxin and receptor structures. Biochemistry 36, 12836–12844.

Antil, S., Servent, D., Ménez, A., 1999. Variability among the sites by which curaremimetic toxins bind to *Torpedo* acetylcholine receptor, as revealed by identification of the functional residues of α-cobratoxin. J. Biol. Chem. 274, 34851–34858.

Basus, V.J., Song, G., Hawrot, E., 1993. NMR solution structure of an α-bungarotoxin/nicotinic receptor peptide complex. Biochemistry 32, 12290–12298.

Cheng, Y.-C., Prusoff, W.H., 1973. Relationship between the inhibition constant (K_i) and the concentration of inhibitor which causes 50% inhibition (IC_{50}) of an enzymatic reaction. Biochem. Pharmacol. 22, 3099–3108.

Corringer, P.J., Galzi, J.L., Eiselé, J.L., Bertrand, S., Changeux, J.P., Bertrand, D., 1995. Identification of a new component of the agonist binding site of the nicotinic α7 homooligomeric receptor. J. Biol. Chem. 270, 11749–11752.

Drevet, P., Lemaire, C., Gasparini, S., ZinnJustin, S., Lajeunesse, E., Ducancel, F., Pinkasfeld, S., Courcon, M., Tremeau, O., Boulain, J.C., Ménez, A., 1997. High-level production and isotope labeling of snake neurotoxins, disulfide-rich proteins. Protein Expression Purif. 10, 293–300.

Eiselé, J.L., Bertrand, S., Galzi, J.L., Devillers-Thiéry, A., Changeux, J.P., Bertrand, D., 1993. Chimaeric nicotinic–serotonergic receptor combines distinct ligand binding and channel specificities. Nature 366, 479–483.

Endo, T., Tamiya, N., 1991. Structure–function relationships of postsynaptic neurotoxins from snake venoms. In: Harvey, A.L. (Ed.), Snake Toxins. Pergamon, NY, pp. 165–222.

Low, B.W., Corfield, P.W.R., 1986. Erabutoxin b: structure/function relationships following initial protein refinement at 0.140-nm resolution. Eur. J. Biochem. 161, 579–587.

Pillet, L., Tremeau, O., Ducancel, F., Drevet, P., Zinn Justin, S., Pinkasfeld, S., Boulain, J.C., Ménez, A., 1993. Genetic engineering of snake toxins. Role of invariant residues in the structural and functional properties of a curaremimetic toxin, as probed by site-directed mutagenesis. J. Biol. Chem. 268, 909–916.

Servent, D., Lamthanh, H., Antil, S., Bertrand, D., Corringer, P.J., Changeux, J.P., Ménez, A., 1998. Functional determinants by which snake and cone snail toxins block the α7 neuronal nicotinic acetylcholine receptors. J. Physiol. (Paris) 92, 107–111.

Servent, D., Winckler-Dietrich, V., Hu, H.Y., Kessler, P., Drevet, P., Bertrand, D., Ménez, A., 1997. Only snake curaremimetic toxins with a fifth disulfide bond have high affinity for the neuronal α7 nicotinic receptor. J. Biol. Chem. 272, 24279–24286.

Trémeau, O., Lemaire, C., Drevet, P., Pinkasfeld, S., Ducancel, F., Boulain, J.C., Ménez, A., 1995. Genetic engineering of snake toxins. The functional site of Erabutoxin a, as delineated by site-directed mutagenesis, includes variant residues. J. Biol. Chem. 270, 9362–9369.

Tsernoglou, D., Petsko, G.A., 1977. Three-dimensional structure of neurotoxin a from venom of the Philippines sea snake. Proc. Natl. Acad. Sci. USA 74, 971–974.

Walkinshaw, M.D., Saenger, W., Maelicke, A., 1980. Three-dimensional structure of the ''long'' neurotoxin from cobra venom. Proc. Natl. Acad. Sci. USA 77, 2400–2404.

Weber, M., Changeux, J.P., 1974. Binding of naja nigricollis [3H] α-toxin to membrane fragments from Electrophorus and *Torpedo* electric organs. Mol. Pharmacol. 10, 15–34.

Zinn Justin, S., Roumestand, C., Gilquin, B., Bontems, F., Ménez, A., Toma, F., 1992. Three-dimensional solution structure of a curaremimetic toxin from *Naja nigricollis* venom: a proton NMR and molecular modeling study. Biochemistry 31, 11335–11347.